

**Subject:** SOI -- Geophysical Assistance

**Date:** 3 September 1996

**To:** Hershel Read  
State Conservationist  
USDA-NRCS  
2121-C 2nd Street, Suite 102  
Davis, California 95616-5475

**PURPOSE:**

The purpose of this study was to use ground-penetrating radar (GPR) techniques to characterize the thickness of weathered bedrock (Cr materials) in granitic terrains.

**PARTICIPANTS:**

Jim Doolittle, Research Soil Scientist, NRCS, Radnor, PA  
Mary Doolittle, Earth Team Volunteer, NRCS, Radnor, PA  
Bob Graham, Professor of Soil Mineralogy, Department of Soils & Environmental Sciences, University of California, Riverside, CA  
Ken Hubert, Graduate Student, Department of Soils & Environmental Sciences, University of California, Riverside, CA  
Susan Southard, Soil Scientist, NRCS, Davis, CA

**ACTIVITIES:**

All field activities were completed during the period of 22 to 26 July 1996.

**BACKGROUND:**

In many west slope areas of the Sierra Nevada Range, California, soil and climatic conditions are relatively harsh for plants. The soil moisture regime is xeric with a pronounced and severe summer dry season. Extensive areas are underlain by coarse- and moderately coarse-textured soils that are shallow (0-50 cm) and moderately deep (50 to 100 cm) to granitic bedrock. These soils have very low available water capacities. Despite these harsh conditions, the biomass within the Chaparral and mixed coniferous ecosystems is considered extraordinary (Jones and Graham, 1993).

It has been determined that weathered bedrock (Cr material) holds a substantial amount of plant-available water (Jones and Graham, 1993; Anderson et al., 1995). In some areas, the amount of plant-available water is greater in the weathered bedrock than in the overlying soil. In the Sierra Nevada Range, the granitic bedrock is highly weathered in the upper part. The Cr material grades with depth into hard, unweathered bedrock (R material). The thickness and characteristics of the Cr material are variable. This weathered material varies in structure, texture, weathering and fracturing qualities (Clayton and Arnold, 1972). Realizing these differences in weathered materials and the inadequacy of present classification schemes, Clayton and Arnold (1972) developed a sequence of weathering classes

for acid igneous rocks. These classes were based on, among other properties, the mechanical strength of the rock, degree of fracturing, and chemical alteration of minerals. These properties affect the ease of root penetration and the available water capacity of Cr material.

Though root restrictive, Cr materials can contain a substantial amount of plant-available water especially along fractures and joints (Jones and Graham, 1993; Anderson et al., 1995). In Southern California, roots have been observed at depths as great as 8.5 m within the rock substrate (Jones and Graham, 1993). The purpose of this investigation was to evaluate the potential of using ground-penetrating radar to chart the depths to Cr and R materials within granitic terrains of the Sierra Nevada Range. Computer graphic techniques were used to display interpreted radar data and characterize spatial patterns existing within a research site.

Ground-penetrating radar is an impulse radar system designed for shallow (0 to 30 m), subsurface investigations. The radar system measures the elapsed time between the transmission and reception of electromagnetic energy. This system operates by transmitting short pulses of high frequency (10-1000 MHz) electromagnetic energy into the ground from an antenna. Each pulse consists of a spectrum of frequencies distributed around the center frequency of the transmitting antenna. Whenever a pulse contacts an interface separating layers of differing electromagnetic properties, a portion of the energy is reflected back to the receiving antenna. The receiving unit amplifies and samples the reflected energy, and converts it into a similarly shaped waveform in a lower frequency range. The processed reflected waveforms can be displayed on a VGA video screen, printed on a thermal recorder, or stored on an internal disk drive for future playback and/or post-processing.

The performance of GPR varied with soil and rock types and from one location to another. Surveys have been most successful in areas where the bedrock is electrically resistive and overlain by a relatively thin (less than 5 m) overburden composed of relatively resistive, coarse or coarse-loamy materials. Stevens and others (1995) reported that observation depths greater than 60 m are possible through electrically resistive, granitic and gneissic rocks. In areas where the overburden is thick or composed of more conductive materials, the depth of observation is frequently too restrictive and the radar fails to provide a continuous profile of the underlying bedrock. Doolittle (1987) reported observation depths of 1 to 2 meters in moderately fine-textured soils and less than 1.5 m in fine textured soils.

Where terrain conditions are appropriate, ground-penetrating radar has been used to map the depths to bedrock (Schellentrager and Doolittle, 1991). It has been used to illustrate soil-bedrock relations on glacial-scoured uplands (Doolittle et al., 1988; Collins et al., 1989) and on karst (Collins et al., 1990 and 1994; Puckett et al., 1990). In areas underlain by different lithologies, GPR has been used to identify and characterize changes in rock types (Benson and Yuhr, 1992; Bjelm et al., 1983, Robillard et al., 1994; Sigurdsson, 1994). This application has been most successful in areas where the underlying lithologies have strongly contrasting electrical properties or internal structure. In bedrock, GPR is sensitive to changes in rock types and fractures (Davis and Annan, 1989). Ground-penetrating radar has been used to detect low-dipping fractures or dikes in bedrock (Davis and Annan, 1989; Holloway and Mugford, 1990, Stevens et al., 1995). Typically, fracture zones have higher moisture and clay contents than the surrounding rock mass. Consequently, these features contrast with the surrounding rock mass and produce strong radar reflections.

In many unglaciated areas, the electrical properties of weathered rock are similar to those of the overlying residual soils and the underlying unweathered bedrock. In these areas it is difficult to identify

the soil/bedrock interface or to differentiate weathered rock from unweathered rock. However, with experience, these reflectors can be recognized on most radar profiles with little ambiguity. Robillard and others (1994) observed that the surface of unweathered bedrock often appears as a continuous reflector of variable amplitude. These researchers' related variations in the amplitude of the reflected signal to differences in rock hardness and mineralogy. Leggo and others (1992) used GPR techniques to distinguish variations in the degree of argillization in granitic bedrock. Robillard and others (1994) observed corestones within more highly weathered bedrock matrix.

### **STUDY SITE:**

The site is located within the Sequoia National Forest in eastern Tulare County, California (Figure 1). The site is near Parker Pass and the headwaters of Starvation Creek. Parker Pass is located in the Greenhorn Mountains of the Sierra Nevada Range. The site is located about 6 kilometers north-northeast of the town of California Hot Springs. The site is mostly forested. Elevations range from about 1960 to 2000 meters. Large outcrops of granite are exposed on the site.

Soils formed principally in residuum weathered from granite bedrock. The upper part of the bedrock has been decomposed by chemical weathering and relatively thick layers of Cr material are present. These layers vary in degree of chemical alteration, fracturing and mechanical strength. The principal soils that have been mapped within the research site are Chaix and Chawanakee. Chaix soils are members of the coarse-loamy, mixed, mesic Dystric Xerochrepts family. Chawanakee soils are members of the loamy, mixed, mesic, shallow Dystric Xerochrepts family. The well drained to somewhat excessively drained Chaix soils are moderately deep over highly weathered bedrock. The somewhat excessively drained Chawanakee soils are shallow over highly weathered bedrock. Both soils have a low available water capacity.

The topography of the study site has been simulated in Figure 2. Relief is about 5.3 m. The research site occupies the summit and upper backslopes of a subordinate ridge, or spur. The spur projects from the side of the mountain range. The spur is not wide and is elongated in a southwest to northeast direction. The summit is flanked by relatively steep slopes. Areas of rock outcrop are conspicuous in the south and southwest portions of the site. In Figure 2, the coordinates are expressed in seconds.<sup>1</sup> These coordinates are based on the Latitude and Longitude grid system. The coordinates for the southwest corner of the study site are 35°57'16" North Latitude and 118°37'39" West Longitude.

## **MATERIALS AND METHODS**

### **Equipment:**

The radar unit used in this study was the Subsurface Interface Radar (SIR) System-2, manufactured by Geophysical Survey Systems, Inc\*. This unit is backpack portable and requires two people to operate. The use and operation of GPR have been discussed by Morey (1974), Doolittle (1987), and Daniels and others (1988). The SIR System-2 consists of a digital control unit (DC-2) with keypad, VGA video screen, and connector panel. The model 3110 (120 mHz), 3105 (300 mHz), and 3102 (500 mHz) antennas were used in this investigation. The radar system was powered by a 12-VDC battery.

<sup>1</sup> Errors in the number of expressed decimal points were noted in the plotted data. Coordinates were expressed in degrees. The small size of the research site required each coordinates express to 1/100000 of a degree. This could not be accomplished in Surfer for Windows. As a consequence, the data were transformed and expressed in 1/10 of a second (latitude and longitude).

The radar profile included in this report was processed through RADAN software. Processing was limited to signal stacking, horizontal scaling, customizing color transform and color tables, and annotations.

All field coordinates were obtained with a Rockwell Precision Lightweight GPS Receiver (PLGR)\*. This receiver was operated using an external power source (portable 9 volt battery). The system was operated in the continuous mode. This mode uses the most power, but acquires and continues to track up to five satellites. Changes in position are continuously shown on the display. Positions were recorded using the Latitude and Longitude coordinates system. Positions were reported in degrees and minutes with a theoretical maximum position resolution of about 2 m. All recorded points had a *figure of magnitude* (FOM) of 1. The selected horizontal datum was the 1927 North American Datum.

To help summarize the results of this study, the SURFER for Windows software, developed by Golden Software, Inc.\*, was used to construct two- and three- dimensional simulations. Grids were created using kriging methods with an octant search. All grids were smoothed using a cubic spline interpolation. In most of the enclosed plots, to help emphasize spatial patterns, filled contour lines have been used. Other than showing trends and patterns, no significance should be attached to the intensity of the filled contours themselves.

### **Field Methods:**

Because of dense vegetation, it was impractical to establish a grid across the study site. Eight traverse lines were established across the site. Five lines (A, B, C, D, and E) were oriented in essentially an east - west direction. Three lines (F, G, and H) were oriented in basically a north - south direction and intersected lines C, D, and E. The eight lines formed a crude grid. These lines varied in length and ranged from about 25 to 60 m. Along each line, survey flags were inserted in the ground at 5 m intervals. This provided 79 observation points. The coordinates of each observation point were approximated with GPS. At each observation point, the relative elevation of the surface was determined with a level and stadia rod. Elevations were not tied to a benchmark; the lowest observation point served as datum. Datum was presumed to be 2000 m.

The GPR survey was conducted by pulling the 300 MHz antenna along each traverse line. Later, traverses were completed with both the 120 and 500 MHz antennas. These ancillary traverses were made to improve the resolution of subsurface features or to clarify interpretations of the depths to Cr and R materials. As these traverses were conducted through a wooded area, all radar traverses were completed with the GPR control unit carried in a backpack and the antenna pulled by hand.

## **RESULTS**

### **GPS Survey:**

---

\* Trade names have been used for informational purposes. Their mention does not constitute endorsement.

\* Trade names have been used for informational purposes. Their mention does not constitute endorsement.

The coordinates of each observation point (79) were obtained from the GPS receiver. Coordinates were expressed in degree minutes. The locations of these points are shown in Figure 3. In Figure 3, each observation point is identified by a letter and a number. The letter signifies the traverse line; the number indicates the observation point along the traverse line. In Figure 3, the coordinates are expressed in seconds.<sup>2</sup> These coordinates are based on the Latitude and Longitude grid system. The coordinates for the southwest corner of the study site are 35°57'16" North Latitude and 118°37'39" West Longitude.

In Figure 3, it is obvious that many of the referenced locations are improperly spaced, misaligned, and incorrectly orientated. Position errors could be attributed to the obstruction of satellite signals by the dense tree cover or higher-lying terrains.

The locations of the observation points were inaccurate. However, these locations were needed to construct computer simulations of the interpreted depths to Cr and R materials. After reviewing Figure 3, it became apparent that several observation points were extremely displaced. These observation points (30) were deleted from the data set. The locations of the remaining observation points (49) were considered more accurately spaced and aligned. These observation points were used to construct all computer simulations found in this report. Figure 4 shows the locations of these observation points.

The plotting of spatial patterns from imprecise coordinates is like the face of a cartoon character that has been copied and distorted by *silly putty*. In the enclosed computer simulations, the locations of the observation points and traverse lines, though imprecise, are considered close approximations. As if *silly putty*, the shape and form of the resultant computer simulations have been distorted. However, it is hoped that general trends can be approximated in the data set. Future studies must insure more accurate ground control.

## Ground-penetrating radar survey:

### A. The radar profile -

Reflected radar waveforms were plotted on a raster-scan, thermal plotter/printer. Through a thermo-chemical reaction, radar images are developed as thermal sensitive paper is moved under a fixed thermal printhead. The intensities of these images are dependent upon the amplitude of the reflected signals. A complete set of the radar profiles has been turned over to Dr. Graham.

Figure 5 is an example of a radar profile. The horizontal scale represents units of distance traveled along an antenna traverse. This scale is dependent upon the speed of antenna advance along a traverse line and the rate of paper advance through the thermal plotter. The vertical scale is a time or depth scale that is based on the velocity of signal propagation.

The four basic components of a radar profile have been identified in Figure 5. These components are the start of scan pulse (A), inherent antenna noise (B), surface image (C), and subsurface interface images (D). Except for the start of scan pulse, these components are generally displayed as a group of dark bands. The number of bands can be limited by high rates of signal attenuation or superimposed signals. These bands limit the ability of GPR to discriminate closely spaced interfaces. The dark bands occur at

<sup>2</sup> Errors in the number of expressed decimal points were noted in the plotted data. Coordinates were expressed in degrees. The small size of the research site required each coordinates express to 1/100000 of a degree. This could not be accomplished in Surfer for Windows. As a consequence, the data were transformed and expressed in 1/10 of a second (latitude and longitude).

both positive and negative signal amplitudes. The narrow white band(s) separating the darker bands represent the neutral or zero crossing between positive and negative signal amplitudes.

The start of scan image (see A in Figure 5) results from direct feed-through of transmitted pulses into the receiver section of the antenna. Though a source of unwanted clutter, the start of scan pulse is often used as a time reference line.

Reflections unique to each of the system's antennas are the first series of multiple bands on radar profiles. Generally the width of these bands increases with decreasing antenna frequency or signal filtration. These reflections (see B in Figure 5) are a source of unwanted noise on radar profiles.

The surface image (see C in Figure 5) represents the ground surface. Below the image of the surface reflection are images from subsurface interfaces (see D in Figure 5). Interfaces can be categorized as being either *plane* or *point reflectors*. Most soil horizons, geologic strata, and fracture traces appear as a series of continuous, parallel bands similar to those appearing in the left-hand portion of Figure 5. Features that produce these reflections are referred to as "*plane reflectors*." Small objects such as rocks, corestones, roots, or buried cultural features can produce a hyperbolic pattern similar to the feature appearing in the right-hand portion of Figure 5. Features that produce these reflections are referred to as "*point reflectors*."

### **B. Calibration -**

Generally, for most soil investigations, auger or coring data, as well as exposures and observation pits, are used to verify interpretations and confirm the depths to known reflectors. These data are used to determine the depth scale(s). At the time of this investigation, five corings were made along a traverse line. These observations were used to scale the radar imagery and to confirm interpretations and observation depths.

The GPR is a time scaled system. This system measures the time that it takes electromagnetic energy to travel from the antenna to an interface (e.g., soil horizon, stratigraphic layer, bedrock surface) and back. To convert the travel time into a depth scale, either the velocity of pulse propagation or the depth to a reflector must be known. The relationships among depth (d), two-way, pulse travel time (t), and velocity of propagation (v) are described in the following equation (Morey, 1974):

$$v = 2d/t$$

The velocity of propagation is principally affected by the relative permittivity or dielectric constant ( $\epsilon$ ) of the profiled material(s) according to the equation:

$$\epsilon = (c/v)^2$$

where c is the velocity of propagation in a vacuum (0.3 m/nanosecond). The velocity is expressed in meters per nanosecond (ns). A nanosecond is one billionth of a second. The amount and physical state of water (temperature dependent) have the greatest effect on the dielectric constant of a material. Tabled values are available that approximate the dielectric constant of some materials (Morey, 1974; Petroy, 1994). However, as discussed by Daniels and others (1988), these values are simply approximations.

Calibration trials were conducted along a traverse line established within the study site. The purposes of the calibration trials were to determine the dielectric constant and velocity of propagation of electromagnetic energy through the soil and Cr material, establish a crude depth scale, verify interpretations, and optimize control and recording settings. Traverses were conducted with the 300 MHz antenna. Considerations of desired versus achievable depths of observation and the resolution of subsurface features influenced the selection of scanning times. The 300 MHz antenna provided a satisfactory balance of resolution and depth of observation.

The augured depths (0.91 to 3.91 m) to R materials at five observation points were used to estimate the velocity of propagation through the soil and Cr materials. As auguring at one of these observation points was halted after coring to 1.68 m, but not to R materials, this observation was not included in the analysis. Based on the round-trip travel time to R material, the averaged velocity of propagation through the soil and Cr materials was estimated to be 0.138 m/ns. The dielectric constant was estimated to be 4.89. The estimated dielectric constant and velocity of propagation were similar to table values reported by Davis and Annan (1989) and Petroy (1994) for granite ( $\epsilon = 4$  to 6;  $v = 0.13$  m/ns). With an average velocity of propagation of 0.138 m/ns, a scanning time of 150 ns provided a maximum observation depth of about 10.3 m.

To confirm the precision of GPR for determining the depths to R material, scaled radar depths were compared with depths observed in four auger observations. At the four observation points, the average observed depth to R material was 2.28 m with a range of 0.91 to 3.91 m. The average difference between the observed and scaled depth to R material was 0.17 m. The correlation between observed and interpreted depths was high ( $r^2 = 0.9476$ ).

### ***C. Radar profiles -***

The 300 and 500 MHz antennas provide adequate observation depths and acceptable resolution of the Cr and R materials. Figure 6 is a representative radar profile from the calibration line. This profile was collected with the 300 MHz antenna. The scanning time was 150 ns. RADAN software was used to stack and normalized this radar profile. Signal stacking can reduce incoherent background noise while enhancing the image of bedrock surfaces. Often, because of noise suppression, stacked traces have considerably more observable features especially at greater depths. Normalization corrects the horizontal scale for variations in the speed of antenna advance along a traverse line. In Figure 6, a dark line has been drawn to emphasize the depth, extent, and characteristics of the inferred upper boundary of the R material.

The horizontal scale represents units of distance traveled along the traverse line. The numbers appearing at the top of the radar profile represent distances in meters. The segmented, vertical lines are observation points and occur at 2 m intervals. The vertical scale is a time or depth scale, which is based on the estimated velocity of signal propagation (0.138 m/ns). In this figure, the depth of observation is about 10 meters (see scale along left-hand margin).

In Figure 6, several subsurface reflectors have been identified. Ground-penetrating radar is an interpretative technique. In areas of multiple or poorly expressed reflectors, interpretations are often plagued by indecision as to which interface should be followed. Without the coring observations, the lower-lying, more strongly expressed interface (B) would have been interpreted as the boundary separating weathered (Cr) from unweathered (R) bedrock.

In Figure 6, the upper-most, continuous subsurface reflector is the boundary separating weathered (Cr) from unweathered (R) bedrock. A dark line has been drawn on the radar profile to emphasize this interface. This interpretation was confirmed by four core observations. The boundary separating weathered from unweathered bedrock is spatially continuous, but it is variable in expression. As it corresponds with the transition from weathering class 3 or 4 materials to weathering class 1 or 2 materials (Clayton and Arnold, 1972), this interface represents a weathering front that is neither abrupt nor highly contrasting. In some portions of this profile, the Cr/R interface is poorly expressed and its exact location is more ambiguous. In all radar profiles, the unweathered bedrock was characterized by the presence and distinct arrangement of high- or medium-amplitude, sub parallel reflectors. These reflectors are believed to represent inherent structure, minerals, or minor fracture traces within the unweathered bedrock. Some are well expressed (B) and may represent veins or major sheeting planes filled with dissimilar materials.

In Figure 6, the Cr material is characterized by the lack of high- or medium-amplitude reflectors. The lack of reflectors is believed to be a manifestation of the weathering processes and the destruction of internal structure. Several forms suggestive of corestones (A) have been identified within the Cr material. These reflectors occur between depths of 1 to 2 meters. Because of the finite resolution of the 300 mHz antenna, features occurring within the upper 40 cm of the soil profile are obscured by the strong surface reflection. Because of the required depth of observation (10 m), features occurring within the upper 1 m of the soil profile are compressed and poorly expressed. As a consequence, the soil/Cr material interface is difficult to discern on this profile (Figure 6).

Figure 7 is a radar profile of the same traverse line shown in Figure 6. This radar profile was collected with the 500 mHz antenna. The scanning time was 60 ns. In this figure, the depth of observation is about 4 meters (see scale along left-hand margin). Compared with Figure 6, the depth of observation is less and the vertical exaggeration is greater in Figure 7. In Figure 7, two parallel intermittent bands of reverberated signals are apparent between depths of 1.5 to 2 meters and 3 to 4 meters. These bands represent unwanted background noise (caused by high signal gain settings).

In Figure 7, the boundary separating weathered (Cr) from unweathered (R) bedrock has been interpreted and charted with a dark line. Several forms suggestive of corestones (A) have been identified within the Cr material. These reflectors occur between depths of 1 to 2 meters. The boundary separating the soil and the weathered (Cr) bedrock has also been interpreted and charted with a dark line. The placement of this line is more interpretative. The 500 mHz antenna provided exceptional resolution of subsurface features. However, the difference in relative permittivity existing between the soil and weathered bedrock was too weak and the boundary separating these layers was too gradational to provide a strong radar reflection. The relative permittivity of the soils was nearly identical with the relative permittivity of the comparatively soft and highly weathered upper part of the Cr material. As a consequence, the boundary separating the soil from the weathered (Cr) bedrock was indistinct, poorly expressed, and difficult to delineation on radar profiles.

Figure 8 is a composite of the radar profiles appearing in figures 7 and 8. Except for distortion caused by differences in vertical exaggeration, these profiles are remarkably similar. These profiles have been stacked and normalized, but have not been annotated. In this study, multiple radar profiles obtained with different antennas, control settings, and depths of observations were used to improve interpretations.

#### ***D. Interpreted Depths to Cr and R materials -***

Attempts to consistently identify the soil/Cr material interface on radar profiles were problematic. Without processing through the RADAN software program, this interface was difficult to distinguish with any degree of reliability. Even with processing, the upper boundary of the Cr material produced weak reflections and indistinct images on most radar profiles. Because of the weak reflection from the soil/Cr material interface, it was assumed that the electromagnetic gradient was gradual and/or dielectric properties were weakly contrasting between these two materials.

The radar survey (with the 300 MHz antenna) was completed in less than one hour. The survey consisted of about 325 meters of continuous radar records. Based on radar interpretations at 79 observation points, the depth to Cr material ranged from about 0.15 to 0.87 m. Within the study site, the average depth to Cr material was about 0.46 m. One-half of the observations had depths to Cr material between 0.35 and 0.54 m. Based on radar interpretations at 79 observation points, the depth to R material ranged from about 1.20 to 6.13 m. The average depth to R material was about 2.66 m. One-half of the observations had depths to R material between 1.84 and 3.17 m. Table 1 summarizes the distribution of soil depths.

**Table 1**  
**Distribution of Depths to R and Cr Materials**  
(ALL MEASUREMENTS ARE IN METERS)

<u>Depth</u>	<u>Frequency (%)</u>	
	<i>Cr Material</i>	<i>R Material</i>
0.0 to 0.5	62%	0%
0.5 to 1.0	38%	0%
1.0 to 1.5	0%	5%
1.5 to 2.0	0%	23%
2.0 to 2.5	0%	23%
2.5 to 3.0	0%	18%
3.0 to 3.5	0%	10%
3.5 to 4.0	0%	8%
4.0 to 4.5	0%	7%
4.5 to 5.0	0%	3%
5.0 to 5.5	0%	1%
5.5 to 6.0	0%	0%
>6.0	0%	1%

Soils within the site were characterized by the radar as being shallow (62 %) and moderately deep (38 %) over weathered bedrock. However, these soils were predominantly very deep (95 %) to unweathered bedrock.

#### ***E. Simulated Plots -***

Figure 9 and 10 are simulations of the depths to Cr and R materials, respectively. In each figure, a two-dimensional plot of either the depths to Cr or R materials have been overlaid upon a three-dimensional surface net diagram of the topography. This technique is useful to illustrate relationships among the soil,

bedrock, and land surface. Color shading and filled contour lines have been used to help emphasize the spatial distribution of these depths.

The depth to Cr material across the research site has been plotted in Figure 9. As illustrated in this figure, depths to Cr material are relatively shallow and invariable across the site. The depth to Cr material ranged from about 0.15 to 0.87 m. The average depth to Cr material was about 0.46 m. Areas of shallow (0 to 50 cm) soil dominate the site, but are more common in the western and southern portions of the site. These areas had the greatest exposure of bedrock outcrops. Areas of moderately deep (50 to 100 cm) soil are more extensive across the eastern portion of the site. Moderately deep soils form a large area that bisects contour lines (see Figure 2) and is essentially orthogonal with the elongated center line of the ridge.

The depth to R material across the research site has been plotted in Figure 10. Depths to R material are mostly very deep (> 150 cm) and highly variable across the site. The depth to R material ranged from about 1.20 to 6.13 m. The average depth to R material was about 2.66 m. Soils that are shallow, moderately deep, and deep to R material comprise only about 5 percent of the site. These soils are observable only in the northeast portion of the site. Areas of very deep soils dominate the site. In Figure 10, shoulder and upper backslopes positions forming the southern and northern flanks of the ridge have soils with conspicuously deeper depths to R material. In these two areas, depths to R material and thickness of Cr materials (see Figure 11) exceed 3 meters.

Figure 11 is a simulation of the thickness of Cr materials within the study site. This plot is closely similar to the plot of the depth to R material (see Figure 10). Areas with thick layers of Cr materials are assumed to have greater plant-available water. Areas with thick layers of C material form conspicuous belts on either side of the summit.

Figure 12 is a composite of surface net diagrams for the soil, Cr material, and R material. This simulation shows that the surfaces of the soil and Cr material are closely similar. The topographies of the soil and Cr material surfaces appear relatively smooth. The surface of the underlying R material is more variable. Except for summit positions, the topography of the unweathered bedrock does not conform to the topography of the soil surface. The topography of R material surface appears notched and irregular.

## CONCLUSIONS:

1. This study demonstrated the utility of using high-resolution, ground-penetrating radar techniques as an aid for interpolation and extrapolation of the data obtain with traditional coring methods. Radar profiles provided a continuous picture of subsurface features that complements traditional coring methods. Ground-penetrating radar provides a noninvasive method for rock mass characterization. Recent developments in GPR technology have resulted in more portable equipment that has enabled surveys in more forbidding and remote terrains.

2. Ground-penetrating radar techniques are noninvasive. Compared with traditional survey methods, GPR techniques are faster and provide greater numbers of observations per unit time. These techniques are therefore more efficient and provide more comprehensive coverage. Ground-penetrating radar can cover large areas at comparatively low costs. This report described procedures for conducting surveys and for displaying data.

3. Ground-penetrating radar techniques appear suitable for pedological investigations in many portions of the Sierra Nevada Range. Ground-penetrating radar was used to characterize rock masses. The radar profiled the subsurface to depths greater than 10 m and provided a continuous record of the thickness of Cr material and depth to R material. The correlation between the observed (soil auger) and the interpreted (GPR) depths to R material was ( $r^2 = 0.9476$ ). The interpreted depth to Cr material averaged 0.46 m with a range of 0.15 to 0.87 m. The interpreted depth to R material averaged 2.66 m with a range of 1.20 to 6.13 m.

4. As far as the use of GPR within the Sierra Nevada Range, additional challenges and needed improvements in field operations will be faced. Future studies will require more accurate ground control. In areas of shallow and moderately deep soils, the soil/Cr material interface was difficult to identify on most radar profiles. Even with processing, the upper boundary of the Cr material produced weak reflections and indistinct images. Additional studies are needed to optimize settings on the control unit and to improve interpretations. Interpretations can only be improved with repeated field studies supported by sufficient "ground truth" verifications.

5. A complete set of radar profiles has been returned to Dr. Graham for use in his research. In addition all radar profiles have been stored on tapes and will be maintained in my office. The examples provided in this report are for general guidance only. Upon request and with advanced notice, select portions of the radar profiles can be processed and made available.

I am very pleased to have had the opportunity to work with Dr. Graham and Ken Hubert of the University of California at Riverside, and Susan Southard of NRCS. We made a good team and I enjoyed working with these people.

With kind regards,

James A. Doolittle  
Research Soil Scientist

cc:

J. Culver, Supervisory Soil Scientist, USDA-NRCS, National Soil Survey Center,  
Federal Building, Room 152, 100 Centennial Mall North, Lincoln,  
NE 68508-3866

B. Graham, Professor of Soil Mineralogy, Department of Soils & Environmental Sciences, 2208  
Geology Bldg., University  
of California, Riverside, CA 92521-0424

S. Southard, Soil Scientist, NRCS, 2121-C 2nd Street, Davis, CA 95616

S. Holzhey, Supervisory Soil Scientist, USDA-NRCS, National Soil Survey Center,  
Federal Building, Room 152, 100 Centennial Mall North, Lincoln,  
NE 68508-3866

D. Smith, West Regional Soil Scientist, NRCS, Sacramento, CA

E. Vinson, State Soil Scientist/MO Leader, NRCS, 2121-C 2nd Street, Davis, CA 95616

## References

- Anderson, M. A., R. C. Graham, G. J. Alyanakian, and D. Z. Martynn. 1995. Late summer water status of soils and weathered bedrock in a giant sequoia grove. *Soil Science* 160(6):415-422.
- Annan, A. P. and J. L. Davis. 1977. Radar range analysis for geologic materials. Report of Activities, Geologic Survey of Canada. Paper 77-1B. p. 117-124.
- Benson, R. and L. Yuhr. 1992. Assessment of bauxite reserves using ground penetrating radar. p. 229-236. IN: P. Hanninen and S. Autio (eds.) Fourth International Conference on Ground-Penetrating Radar. 7 to 12 June 1992. Rovaniemi, Finland. Geological Survey of Finland, Special Paper 16. pp. 365.
- Bjelm, L., S. Folin, and C Svensson. 1983. A radar in geological subsurface investigation. *Bulletin of the International Association of Engineering Geology*. 26-27:10-14.
- Clayton, J. L., and J. F. Arnold. 1972. Practical grain size, fracturing density and weathering classification of intrusive rocks in the Idaho batholith. USDA Forest Service General Technical Report INT-2 Intermountain Forest Range Experiment Station, Ogden, Utah. p. 17.
- Collins, M. E., J. A. Doolittle, and R. V. Rourke. 1989. Mapping depth to bedrock on a glaciated landscape with ground-penetrating radar. *Soil Science Society of America J.* 53:1806-1812.
- Collins, M. E., W. E. Puckett, G. W. Schellentrager, and N. A. Yust. 1990. Using GPR for micro-analyses of soils and karst features on the Chiefland Limestone Plain in Florida. *Geoderma* 47:159-170.
- Collins, M. E., M. Crum, and P. Hanninen. 1994. Using ground-penetrating radar to investigate a subsurface karst landscape in north-central Florida. *Geoderma* 61:1-15.
- Daniels, D. J., D. J. Gunton, and H. F. Scott. 1988. Introduction to subsurface radar. *IEE Proceedings* 135F(4):278-320.
- Davis, J. L. and A. P. Annan. 1989. Ground-penetrating radar for high resolution mapping of soil and rock stratigraphy. *Geophysical Prospecting* 37:531-551.
- Doolittle, J. A. 1987. Using ground-penetrating radar to increase the quality and efficiency of soil surveys. IN *Soil Survey Techniques*, Soil Sci. Soc. Am. Special Pub. No 20. pp. 11-32.
- Doolittle, J. A., R. A. Rebertus, G. B. Jordan, E. I. Swenson, and W. H. Taylor. 1988. Improving soil-landscape models by systematic sampling with ground-penetrating radar. *Soil Survey Horizons*. 29(2):46-54.
- Holloway, A. L. and J. C. Mugford. 1990. Fracture characterization in granite using ground probing radar. *CIM Bulletin* 83(940):61-70.
- Jones, D. P. and R. C. Graham. 1993. Water-holding characteristics of weathered granitic rock in chaparral and forest ecosystems. *Soil Science Society of America J.* 57:256-261.

Leggo, P. J., J. M. Glover, and M. R. Wajzer. 1992. The detection and mapping of kaolinitic clay by ground probing radar in the Cornish granites of southwest England. pp. 205-215. IN: P. Hanninen and S. Autio (eds.) Fourth International Conference on Ground-Penetrating Radar. 7 to 12 June 1992. Rovaniemi, Finland. Geological Survey of Finland, Special Paper 16. pp. 365.

Morey, R. M. 1974. Continuous subsurface profiling by impulse radar. pp. 212-232. IN: Proceedings, ASCE Engineering Foundation Conference on Subsurface Exploration for Underground Excavations and Heavy Construction, held at Henniker, New Hampshire. Aug. 11-16, 1974.

Petroy, D. E. 1994. Assessment of ground-penetrating radar applicability to specific site investigations: Simple methods for pre-survey estimation of likely dielectric constants, target resolution and reflection strengths. SAGEEP 94. Symposium on the Application of Geophysics to Engineering and Environmental Problems. 27 to 31 March 1994. Boston, Massachusetts. pp. 21.

Puckett, W. E., M. E. Collins, and G. W. Schellentrager. 1990. Design of soil map units on a karst area in West Central Florida. Soil Science Society of America J. 54:1068-1073.

Robillard, C. P. Nicolas, P. Armirat, M. Gariepy, and F. Goupil. 1994. Shallow Bedrock profiling using GPR. p. 1167-1179. IN: GPR 94. Proceedings of the Fifth International Conference on Ground Penetrating Radar. 12 to 16 June 1994. Kitchener, Ontario, Canada. Waterloo Center for Groundwater Research. pp. 1294.

Schellentrager, G. W. and J. A. Doolittle. 1991. Systematic sampling using ground-penetrating radar to study regional variation of a soil map unit. Chapter 12. p. 199-214. IN: Mausbach, M. J., and L. P. Wilding (eds.). Spatial Variabilities of Soils and Landforms. Soil Science Society of America Special Publication No. 28. pp. 270.

Sigurdsson, T. 1994. Application of GPR for geological mapping, exploration of industrial mineralization and sulphide deposits p. 941-955. IN: GPR 94. Proceedings of the Fifth International Conference on Ground Penetrating Radar. 12 to 16 June 1994. Kitchener, Ontario, Canada. Waterloo Center for Groundwater Research. pp. 1294.

Stevens, K. M., G. S. Lodha, A. L. Holloway, and N. M. Soonawala. 1995. The application of ground-penetrating radar for mapping fractures in plutonic rocks within the Whiteshell Research Area, Pinawa, Manitoba, Canada. Journal of Applied Geophysics. 33:125-141.

**PARKER PASS RESEARCH SITE  
SEQUOIA NATIONAL FOREST  
TULARE COUNTY, CALIFORNIA  
RELATIVE TOPOGRAPHY  
(CONTOUR INTERVAL = 0.5 M)**

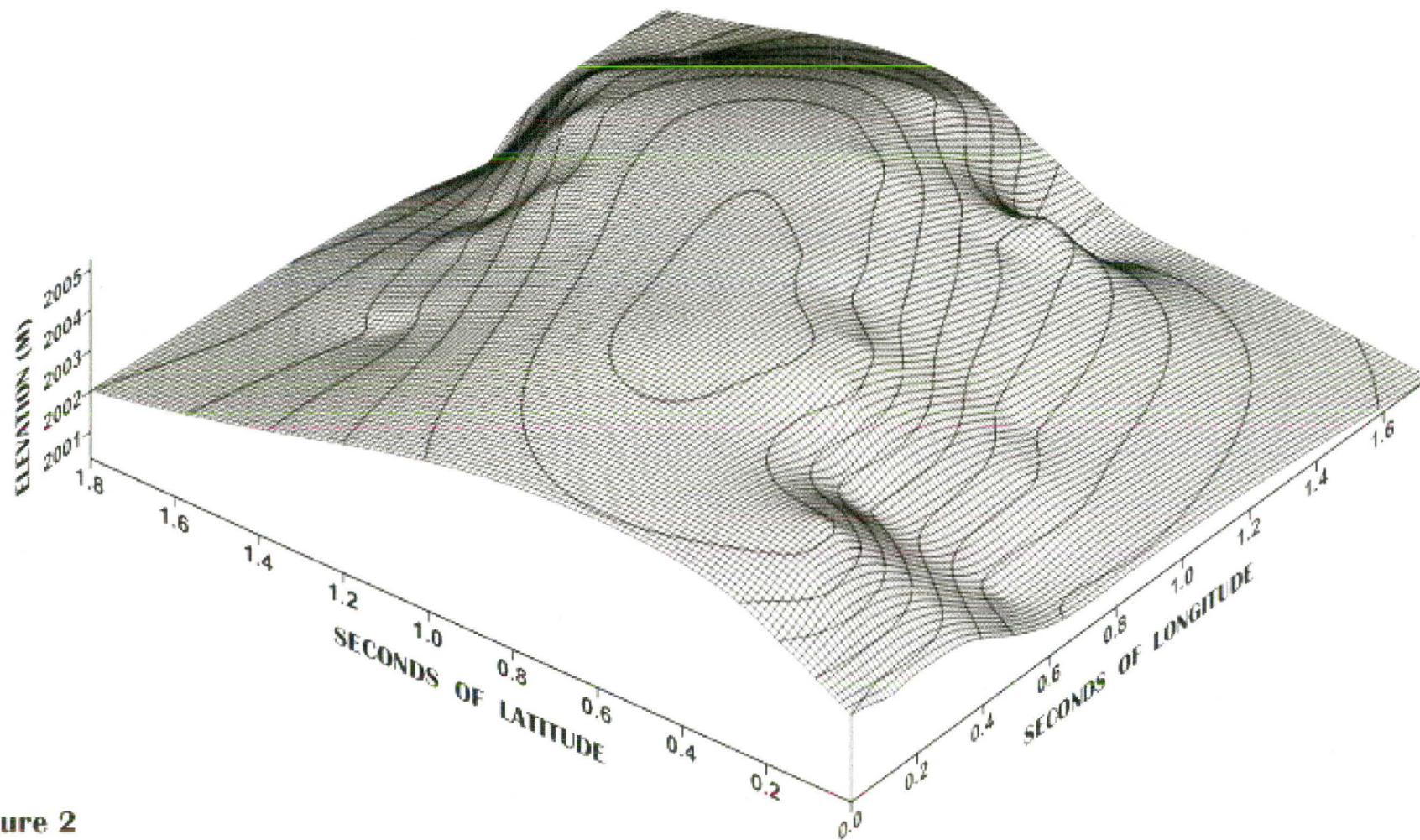
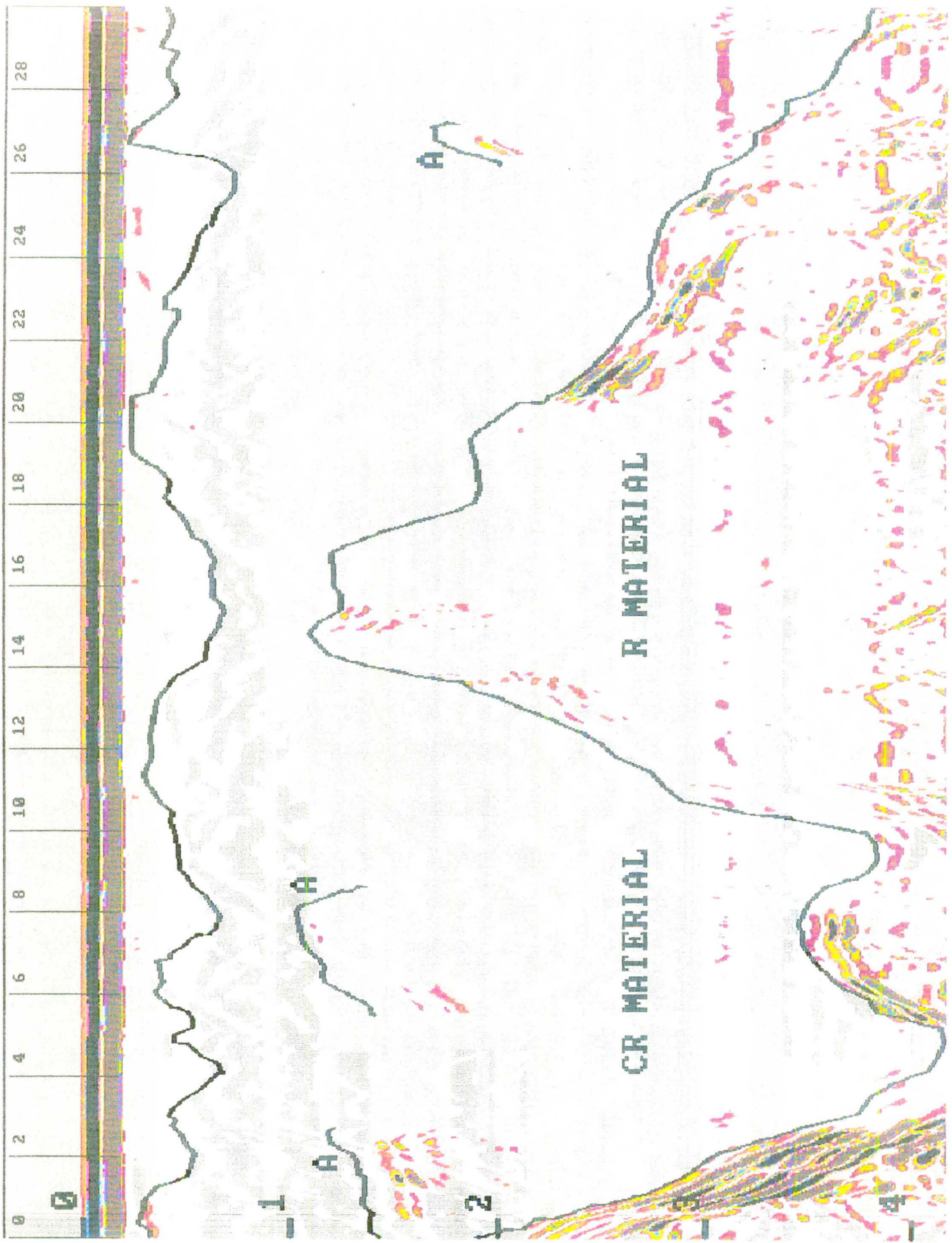


**Figure 2**



**PARKER PASS RESEARCH SITE  
SEQUOIA NATIONAL FOREST  
TULARE COUNTY, CALIFORNIA  
DEPTH TO Cr MATERIAL**

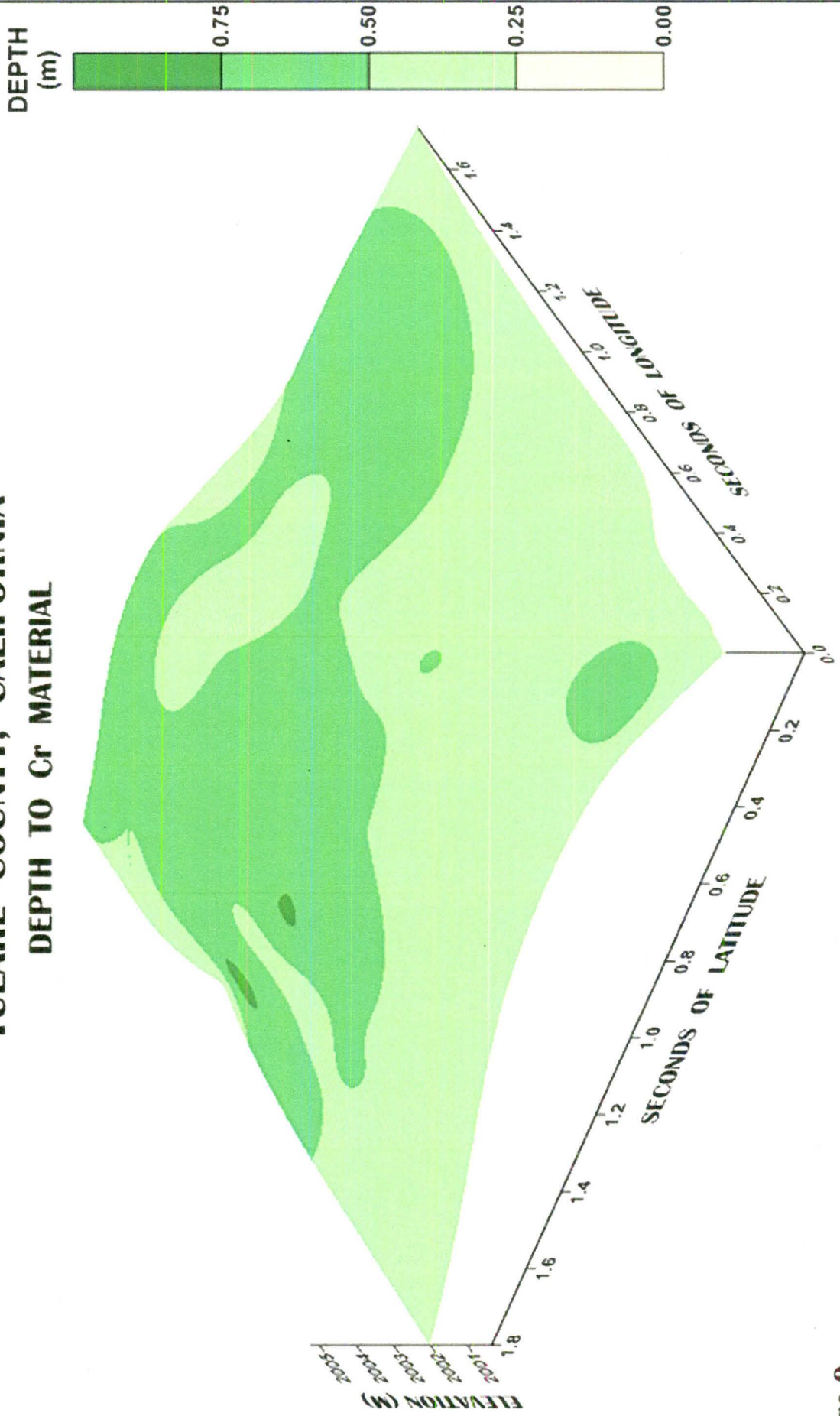


**Figure 9**

**PARKER PASS RESEARCH SITE  
SEQUOIA NATIONAL FOREST  
TULARE COUNTY, CALIFORNIA  
DEPTH TO R MATERIAL**

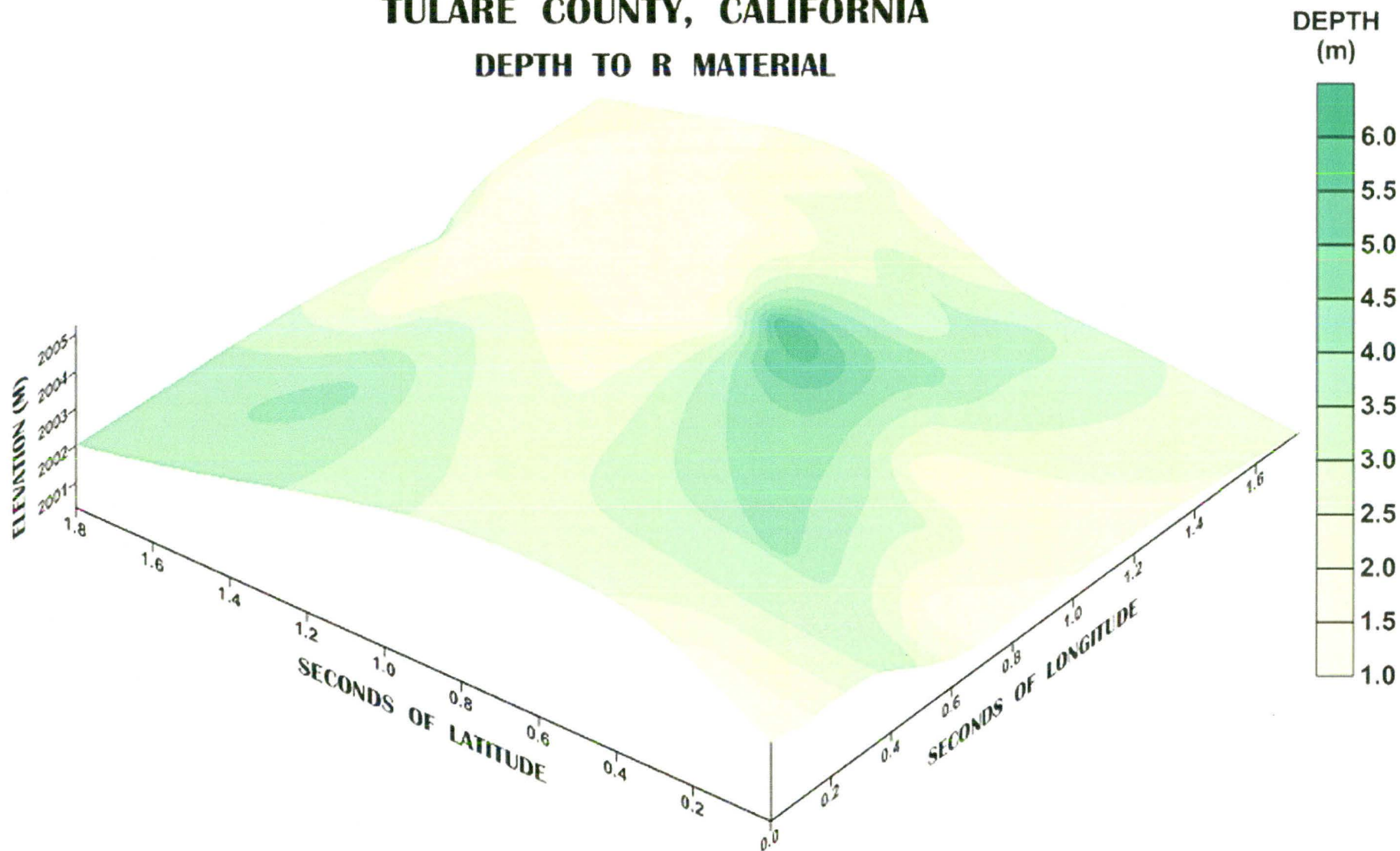


**Figure 10**

**PARKER PASS RESEARCH SITE  
SEQUOIA NATIONAL FOREST  
TULARE COUNTY, CALIFORNIA  
THICKNESS OF Cr MATERIAL**

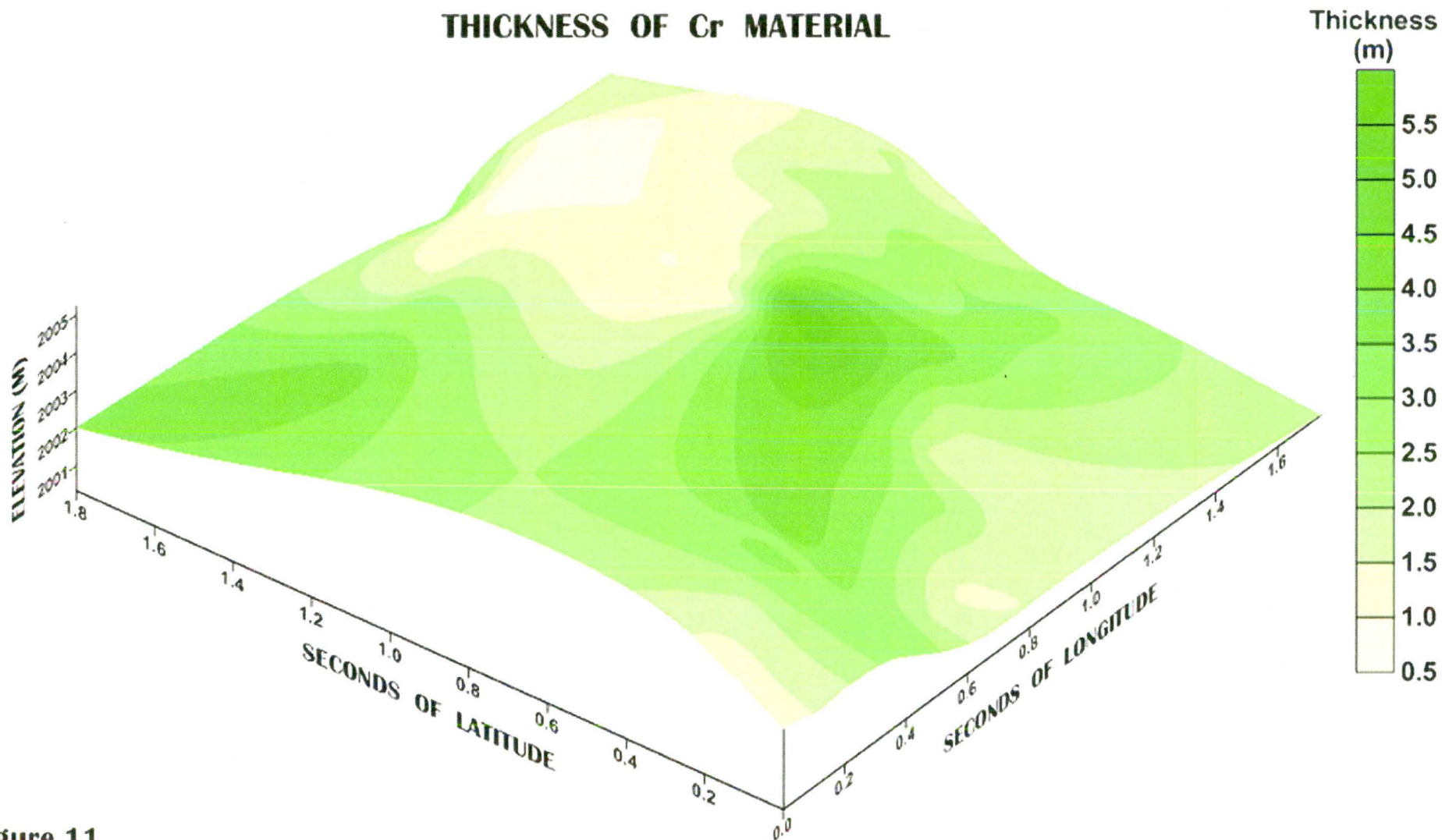


**Figure 11**

**PARKER PASS RESEARCH SITE  
SEQUOIA NATIONAL FOREST  
TULARE COUNTY, CALIFORNIA**

**Relative Surface Topography  
for the  
Soil, Cr, and R Materials**

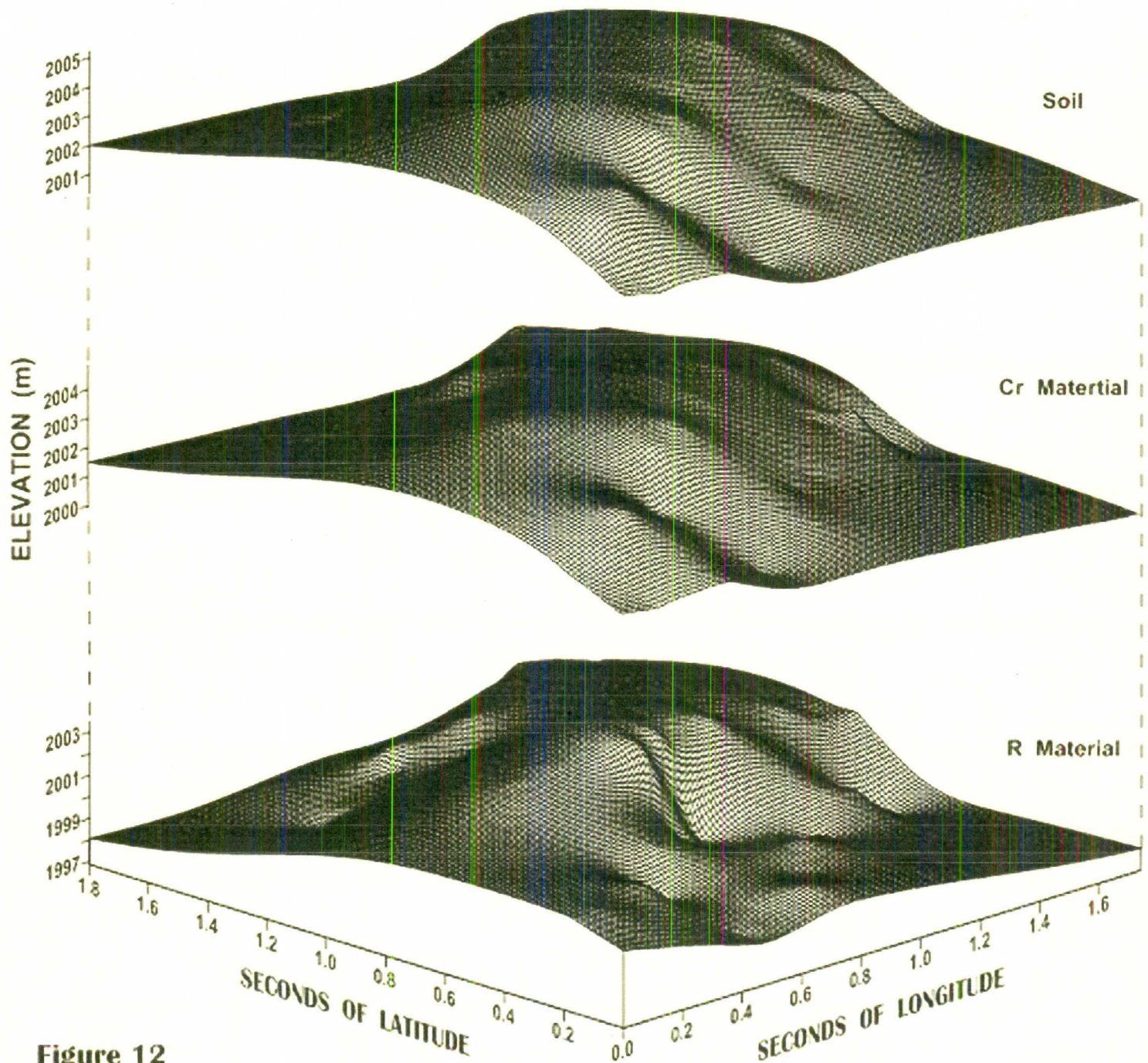


**Figure 12**